Double-ionization mechanisms of the argon dimer in intense laser fields

B. Ulrich,[1] A. Vredenborg,[1] A. Malakzadeh,[1] M. Meckel,[1] K. Cole,[1] M. Smolarski,[2] Z. Chang,[3] T. Jahnke,[1] and R. Dörner[1,*]

[1]*Institut für Kernphysik, Goethe Universität, Max-von-Laue-Strasse 1, D-60486 Frankfurt, Germany*
[2]*Department Physik, ETH Zürich, Wolfgang-Pauli-Strasse 16, CH-8093 Zürich, Switzerland*
[3]*Physics Department, Kansas State University, 116 Cardwell Hall, Manhattan, Kansas 66506, USA*

We have measured the two-site double ionization of argon dimers by ultrashort laser pulses leading to fragmentation into two singly charged argon ions. Contrary to the expectations from a pure Coulomb explosion following rapid removal of one electron from each of the atoms, we find three distinct peaks in the kinetic energy release (KER) distribution. By measuring the angular distribution of the fragment ions and the vector momentum of one of the emitted electrons for circular and linear laser polarization, we are able to unravel the ionization mechanisms leading to the three features in the KER. The most abundant one results from tunnel ionization at one site followed by charge-enhanced tunnel ionization of the second atom. The second mechanism, which leads to a higher KER we identify as sequential tunnel ionization of both atoms accompanied by excitation. The third mechanism is present with linearly polarized light only. It is most likely a frustrated triple ionization, where the third electron does not escape but is trapped in a Rydberg state.

PACS number(s): 32.80.Rm, 32.80.Wr

I. INTRODUCTION

The attractive van der Waals force gives rise to bound states for diatomic molecules of all noble gases. For argon dimers a binding energy of 12.3 meV (99.2 cm^{-1}) and an equilibrium internuclear distance of $R_{Ar_2} = 3.761(3)$ Å have been determined [1,2]. Due to its large internuclear distance the overlap of the atomic orbitals is negligible and outer electrons stay localized at their nucleus in contrast to covalently bound molecules. From the electronic structure point of view, rare-gas dimers resemble very closely two separated neighboring atoms.

This feature makes rare-gas dimers a very attractive species for the study of their interaction with strong laser fields. The multiple-ionization dynamics can be compared to the much studied atomic case (see [3,4] and references therein) and yet phenomena found typically in molecular photo ionization can be expected as well. In the present article we focus on two-center double ionization of the argon dimer and try to unravel by which mechanisms two Ar$^+$ ions are created in the laser field. The atoms in these van der Waals molecules are ionized and the repulsion of the charges induces Coulomb explosion. For the most simple case of two-point charges the kinetic energy release (KER) is inversely proportional to the distance between the atoms.

Double ionization of atoms in a laser field can proceed sequentially by two independent interactions with the laser field or alternatively in a nonsequential manner. For argon atoms at the intensities used here it is well established that nonsequential double ionization proceeds mainly via rescattering [5]. For molecules, Seideman *et al.* [6] has shown that there is a qualitative new mechanism for double ionization. When the electric field of a laser pulse is aligned along the internuclear axis it bends the molecular potential in such a way that there is an enhanced probability of one of the electrons to tunnel out over the internuclear barrier. The effect was called

charged-resonance-enhanced ionization (CREI) by Zuo and Bandrauk [7] and is observed for longer bond lengths during the dissociation process in the hydrogen molecule. The bond lengths where CREI is observed are similar to the bond lengths of the neutral argon dimer and therefore a similar effect could be expected. CREI has a strong angular dependence, as the highest probability is found when the molecular axis is parallel to the electric-field vector [8].

In our experiment we detected the vector momenta of both ions and one of the electrons in coincidence. We will describe this in more detail in the experimental section. This multiple coincidence measurement gives us a wealth of information on the ionization processes. One of the most striking and surprising findings which we will describe in the results sections are three distinct peaks in the KER. They show that a simple Coulomb explosion is not the only fragmentation process in the strong field. In the discussion section we compile all our experimental evidences, like angular distributions of ions and electrons, to unravel the three different mechanisms leading to these peaks.

II. EXPERIMENT

A femtosecond multipass amplified Ti:sapphire laser (KM-Labs Dragon) is employed for double ionization of argon dimers with a mean wavelength of 790 nm at 8 kHz repetition rate and a temporal pulse width of 35 fs. The laser polarization was modified by a half-wave plate and a quarter-wave plate to rotate the linear polarization and switch to circular polarization, respectively. The laser beam was focused by a parabolic mirror with a 7.5-cm focal length onto a supersonic gas jet. The laser peak intensity was determined by the ratio of Ar^{2+}/Ar$^+$ [9] and the branching ratios of H$_2^+$ dissociation channels [10] for linear polarization and by measuring the electron momentum for the case of circularly polarized light [11].

We used a standard cold target recoil ion momentum spectroscopy (COLTRIMS) setup described in detail in [12,13] to measure the three-dimensional (3D) momentum vectors of

*Doerner@atom.uni-frankfurt.de

electrons and ions in coincidence. Electrons and ions were guided by a homogenous electric field of 8 V/cm and a magnetic field of 6.4 G toward two time- and position-sensitive detectors consisting of multichannel plates and a multihit-capable delay-line anode for position readout. On the electron side we used a so-called *Hexanode* detector featuring three delay-line layers to improve the multihit performance [14]. From the time-of-flight (TOF) and the position of impact on the detector the 3D momentum vector was obtained for each particle.

As a source for argon dimers a supersonic jet was generated by driving argon gas through a 30-μm nozzle at a pressure of 2 bar. The supersonic jet entered the interaction chamber through a skimmer 0.3 mm in diameter. The parameters of our supersonic expansion were chosen such that most of the beam consisted of monomers with a fraction of about 1%–2% of dimers and a much smaller fraction of larger clusters. Laser power was adjusted to yield an intensity of 3×10^{14} W/cm^2 for linearly polarized light such that only about 2 ions per shot were created. For circular polarization, intensity was tuned to obtain the same peak field strength as for linear polarization. Most measured ionization events were caused by Ar monomers. To distinguish Coulomb exploded Ar$_2$ clusters from random coincidences of two monomers created in the same pulse, we restricted the kinetic energy release of the fragments to be >1 eV in the off-line analysis. In addition, for a two-ion coincidence event to be valid, we required the center-of-mass momentum of the ions to be $|p_{\rm cm}| <$ 10 a.u. This procedure also allowed us to suppress background from trimer events where only two ion fragments were detected.

The photo-ion photo-ion coincidence (PIPICO) spectrum in Fig. 1 gives an overview of all ion species detected with linear polarization at an intensity of 3×10^{14} W/cm^2. In this spectrum all combinations of two charged fragments measured in coincidence are shown by plotting the time-of-flight of the first ion versus the time-of-flight of the second

ion. The spectrum reveals a strong yield along a curved line corresponding to the symmetric Ar$^+$-Ar$^+$ breakup as well as two crossing lines corresponding to the asymmetric Ar^{2+}-Ar$^+$ breakup. The remaining vertical and horizontal lines are due to random coincidences resulting from the detection of two ions created during a single laser pulse but coming from residual gas and argon monomers. In this article we will focus on the Ar$^+$ + Ar$^+$ two-center double ionization channel.

III. RESULTS

In Fig. 2 we show a density plot of the magnitude of the vector momentum sum corresponding to the two Ar$^+$ ions versus their KER. This spectrum allows us to distinguish real coincidences from random ones and select only the former for further analysis. If two ions originate from the same argon dimer, their sum momentum will be close to zero and their KER resulting from Coulomb explosion will be higher than 1 eV. Thus, real coincidences lie in a stripe near zero sum

FIG. 2. (Color online) Density plot of the magnitude of the vector momentum sum of the two Ar$^+$ ions versus their KER for linear polarization (upper panel) and circular polarization (lower panel). Coincident Ar$^+$ ions are situated close to zero and thus real coincidences can be distinguished from random ones.
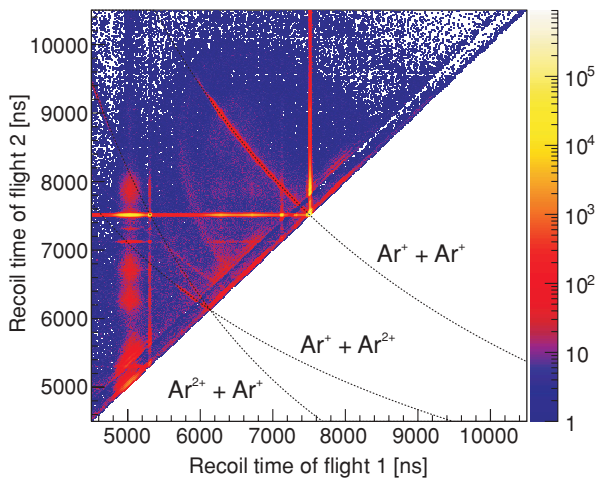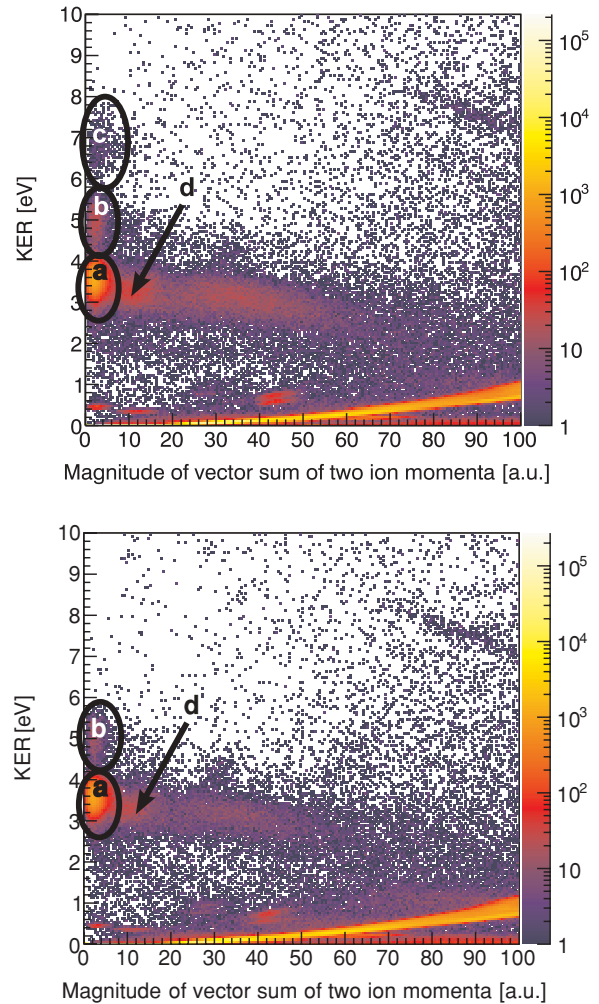

FIG. 1. (Color online) The photo-ion photo-ion coincidence (PIPICO) spectrum for an argon dimer in linear polarized light at an intensity of 3×10^{14} W/cm^2. The Ar$^+$-Ar$^+$ breakup is the most efficient decay channel. The corresponding spectrum from circular polarization looks the same.
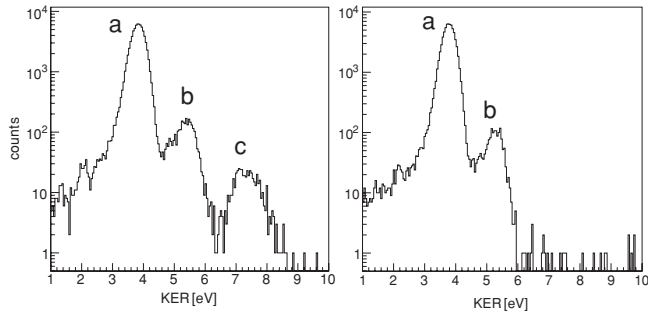
FIG. 3. KER distribution of Ar$^+$ ions for the case of linear polarization and an intensity of 3×10^{14} W/cm^2 (left panel) and for circular polarization with the intensity adjusted to the same peak field strength (right panel). For linear polarization three distinct peaks can be distinguished at 3.8, 5.3, and 7.3 eV, whereas for circular polarization the highest KER peak at 7.3 eV disappears.

momentum. However, we are unable to completely exclude contamination by Ar$_3$ dissociating into two singly charged and a neutral argon atom with very small momentum. These events appear as a stripe at 3.9 eV and are located in the area marked with a "d."

The upper panel of Fig. 2 shows the results for linearly polarized light. The spectrum reveals three features, marked "a," "b," and "c," originating from dimer breakup. On the lower panel the same plot is shown for circular polarization. It is immediately visible that the feature "c" with the highest energy in the case of linearly polarized light disappears for circularly polarized light whereas the other peak structures remain unchanged.

In Fig. 3, the KER distribution for linear polarization (left panel) and circular polarization (right panel) are shown. These are extracted from Fig. 2 by selecting only events with a center-of-mass momentum of <10 a.u. Both distributions are normalized to the respective number of singly ionized argon atoms for comparison. We present the number of observed events for distinct channels in Table I. In order to make the data for linearly and circularly polarized light comparable, we normalize all values to the number of Ar$^+$ from monomers detected with linear polarization. The KER distribution from linear polarization shows three peaks, with the dominant peak at 3.8 eV and two weaker peaks at 5.3 and 7.3 eV. Again, the same dominant peak at 3.8 eV is observed for circularly polarized light, but only the weaker peak at 5.3 eV appears and the highest KER peak at 7.3 eV has disappeared compared to the linearly polarized laser light.

TABLE I. Comparison of ion yields from circularly and linearly polarized light. All values were normalized to the yield of Ar$^+$ monomers from linearly polarized light.

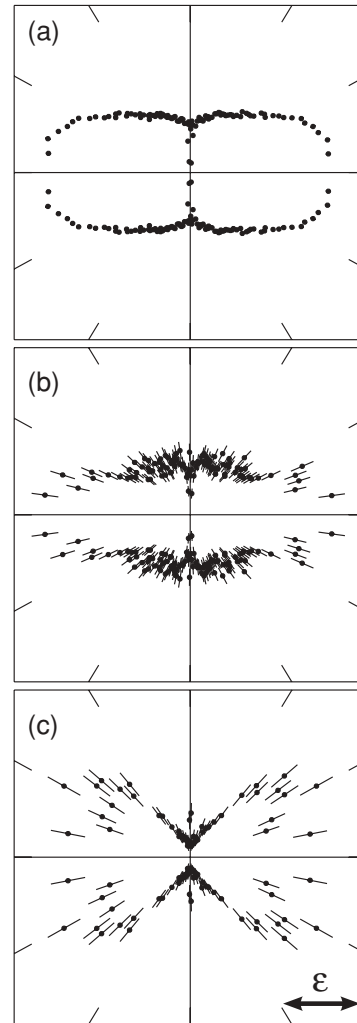| Ions	Linear	Circular	Ratio
Ar$^+$ monomer	3 679 059	3 679 059	:=1
Ar^{2+} monomer	161 461	11 348	$\approx$14.23
Ar$^+$ + Ar$^+$ total	80 315	71 801	$\approx$1.12
Ar$^+$ + Ar$^+$ channel a	76 913	70 212	$\approx$1.10
Ar$^+$ + Ar$^+$ channel b	2839	1589	$\approx$1.80
Ar$^+$ + Ar$^+$ channel c	563	–	–

FIG. 4. Polar plots of angular distributions of Ar$^+$-Ar$^+$ for the corresponding peaks (a–c) of Fig. 3. All channels exhibit an enhanced ionization probability along the polarization direction. Before ionization, the angular distribution of dimer axes is isotropic. The ionizing radiation is linearly polarized along the horizontal axis.

The three distinct channels observed in the KER distribution of Fig. 3 will be discussed independently in the following section. However, before proceeding to the discussion, the polar plots of the ion angular distribution are presented for each KER peak for linear laser polarization in Fig. 4 with the polarization oriented horizontally. The three angular distributions show a preferential direction for the dimer to break up in parallel with the laser polarization vector. Note that the laser pulse is 35 fs, which is too short for an alignment of the argon dimer to occur.

IV. DISCUSSION

A. Peak (a)

The KER of peak (a) is consistent with Coulomb explosion of two-point charges starting from the ground-state internuclear distance of the argon dimer. Assuming a $1/R$ potential we obtain an internuclear distance of 3.9 Å for peak (a). This

is very close to the equilibrium bond length of the neutral dimer. Hence, the ejection of the two electrons must occur via a fast process that does not give the nuclei significant time to move.

In the following we discuss the nature of this ultrafast double-ionization process. For atoms, double ionization is known to proceed in either a sequential or a nonsequential way mediated by rescattering [5]. In the rescattering scenario one electron is tunnel ionized, accelerated, and driven back by the optical field to its parent ion where it knocks out a second electron in an $(e,2e)$ type collision. There are three well-established signatures allowing one to distinguish sequential double ionization from rescattering. First, rescattering leads to a kneelike structure in the intensity dependence of the double-ionization rate [15]. We have not measured the intensity dependence of the signal in peak (a) and hence cannot use that signature. However, the intensity of our experiment is in the range where rescattering double ionization is significant for argon monomers [9]. Second, rescattering-mediated double ionization shows a strong polarization dependence [16], since the laser-driven electron trajectories return to the parent ion only for a linearly polarized field. Third, rescattering-induced double ionization leads to a "double hump" structure in the momentum component of the doubly charged ion parallel to the laser field [9,17,18]. These high momenta result from the doubly charged ion being created close to the zero crossing of the field, when the recolliding electrons have their maximum energy.

Signature two and three both show that double ionization of the monomer at our intensities does proceed via rescattering (see also, e.g., [9]). The Ar^{2+} rate of the monomer shows a very strong elipticity dependence (Table I) and the parallel momentum shows the characteristic "double-hump" structure (Fig. 5, blue dashed line). In contrast to that, the two-center double-ionization peak (a) of the dimer does not show any significant polarization dependence (Table I), ruling out
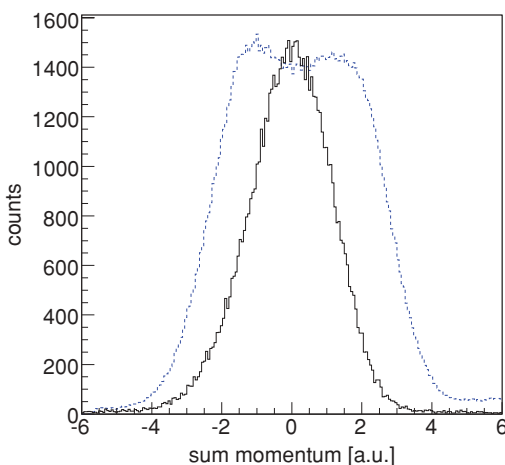

FIG. 5. (Color online) Blue dashed line: Spectrum of the ion momentum of the Ar^{2+} monomer projected onto the z axis (along the polarization direction) for linearly polarized light. The double-hump signature of Ar^{2+} indicates nonsequential ionization; the sum momentum of the argon dimer shows strong evidence for sequential ionization. Black solid line: Sum of the coincident Ar^+ ion momenta of the argon dimer projected onto the z axis.

rescattering. This conclusion is supported also by the parallel-ion sum momentum shown in Fig. 5 by the black solid line. It is a Gaussian centered at zero with a width much narrower than that of the doubly charged monomer. The peak located at zero shows that both electrons are set free close to the maximum of the oscillating field, as is typical for sequential tunneling [9].

Having established sequential tunneling as the mechanism producing peak (a), we now investigate if this sequential tunneling is influenced by the two-center geometry of the dimer. Figure 4 shows that the dimer double-ionization probability is strongly enhanced if the dimer axis is aligned along the polarization direction. For the first ionization step we do not expect any significant dependence on the molecular axis, as the two atoms have negligible electronic overlap and the electronic structure is very close to that of two argon atoms. The removal of the second electron is, however, significantly influenced by the neighboring ion. Such a behavior is known from enhanced ionization or CREI [7]. The ionization of the atom proceeds by tunneling through the barrier created by the atomic potential and the laser field. This barrier is significantly lowered and hence the tunneling increased if a positively charged particle is located on the lower potential side of the field. This enhanced ionization process is highly directional and works only if the molecular axis is parallel to the laser field. Our Fig. 4 shows this behavior.

A second experimental approach to see that directionality of the electron ejection for enhanced ionization is to investigate the electrons directly for the case of circularly polarized light [19]. In the case of circular polarization, the direction of the final electron momentum is (in a simplified model) perpendicular to the electric field of the light at the instant of tunneling. The angular distribution of the final electron momenta in the molecular frame therefore provides information about the angular-dependent ionization probability. In Fig. 6 we show the angular distribution of electrons in the molecular frame for circular light. The internuclear axis of the argon dimer lies horizontally, as depicted by the icon. The distribution exhibits a strong enhancement perpendicular to the dimer axis. As the electronic overlap between the atoms is negligible, the ionization of the first electron will not depend on the axis. In Fig. 6 the angular distribution of the first electron reaching the detector is plotted. Concerning the two steps of the ionization process, this has an equal contribution of "first" and "second" tunneled electrons. Thus, the distribution shown in Fig. 6 consists of 50% isotropically distributed first electrons and 50% second electrons. Only the latter cause the observed anisotropic structure maximizing at 90°. In the lower right panel of Fig. 6 we subtracted the isotropic contribution of the first electron. This electron angular distribution supports the conclusion drawn previously, that the second ionization step proceeds most efficiently at instances when the rotating electric field is parallel to the molecular axis, providing a clear signature of enhanced ionization. We note that the electron distribution is slightly tilted from the normal to the molecular axis. This is an indication of a limitation of the simplified model which neglects the influence of the Coulomb charge on the electron trajectories. It is the joint action of the Coulomb charge and the rotating laser field which leads to the tilt [20].
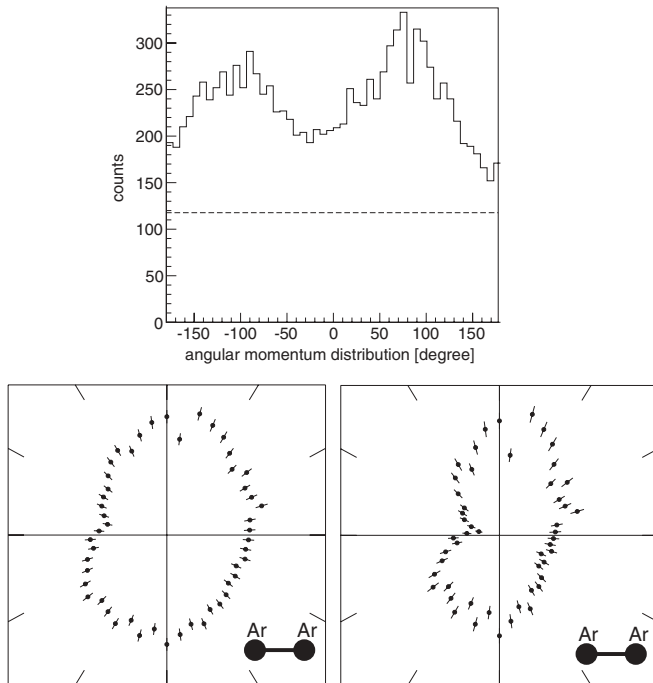
FIG. 6. Angular distribution of one of the two electrons in the molecular frame for circularly polarized light. The emission of the electrons is strongly enhanced when the rotating electric field is parallel to the molecular axis leading finally to an electron angular distribution that peaks perpendicularly to the dimer axis. Upper panel, the dashed line indicates the isotropic contribution of the electron removed first; lower left panel, polar plot of the same data; lower right panel, polar plot of the angular distribution after substraction of the isotropic contribution of the first electron.

B. Peak (b)

Assuming an instantaneous Coulomb explosion of the argon dimer we obtain an internuclear distance R of 2.8 Å for the second KER peak (b) in Fig. 3. This is significantly less than the equilibrium bond length and impossible to reach within a 35-fs laser pulse for an argon dimer starting to contract from its equilibrium bond length [21]. In the following we discuss three possible mechanisms which could produce the surprisingly high KER of peak (b).

(1) Interatomic Coulombic decay (ICD). Single-center ionization plus excitation followed by emission of a second electron via ICD after contraction of the dimer. In this case the final dissociation of the Ar^+-Ar^+ would occur on a potential energy curve of approximately $1/R$ shape, but from a distance smaller than the Ar_2 equilibrium.

(2) Radiative charge transfer (RCT). Single-center double ionization followed by RCT after contraction of the dimer. As in ICD, the final dissociation of the Ar^+-Ar^+ would occur on a potential energy curve of approximately $1/R$ shape, but from a distance smaller than the Ar_2 equilibrium.

(3) Two-center ionization to a highly excited state (excitation). In this case the final dissociation would occur from the equilibrium distance but along a potential curve much steeper than $1/R$.

We will show that our data allow one to conclusively rule out ICD leaving the RCT and the production of highly excited Ar^{+*}-Ar^+ as possible scenarios.

We first discuss the ICD scenario. ICD is a prominent decay channel in loosely bound systems predicted first in pioneering work of Cederbaum and co-workers [22]. In this process an excited ion relaxes by transferring its energy via a virtual photon exchange to a neutral neighbor where this energy leads to ejection of an electron. ICD is well established for rare-gas clusters (see, e.g., [23–27]). The intermediate singly charged excited dimer potential energy curves are often attractive and ICD is preceded by contractive nuclear motion [27–30]. Therefore the kinetic energy release after ICD is often higher than what one would expect from Coulomb explosion from the neutral dimer internuclear distance. Due to the heavy mass of Ar_2 the contraction necessary to result in the observed KER would, however, take much longer than the duration of the laser pulse. So, in the ICD scenario the ICD electron would be emitted after the laser pulse has faded away. To test this experimentally, in Fig. 7, we plot the electron momentum distribution recorded in coincidence with KER peak (b) using circularly polarized light. In a circularly polarized laser field the electrons that are set free during the pulse are driven by the field. They acquire a drift momentum in the plane of polarization [31] and end up on a donut-shaped region in momentum space. They can easily be distinguished from electrons that are released when the laser pulse has already faded away. Figure 7 shows this donut-shaped structure, suggesting that all electrons are set free during the pulse, definitely ruling out the ICD scenario for peak (b). This conclusion is also supported by the preferential breakup along the polarization vector for linear polarized light [Fig. 4(b)]. In the ICD scenario the laser field would have to act only on one atom; therefore no orientation dependence would be expected.
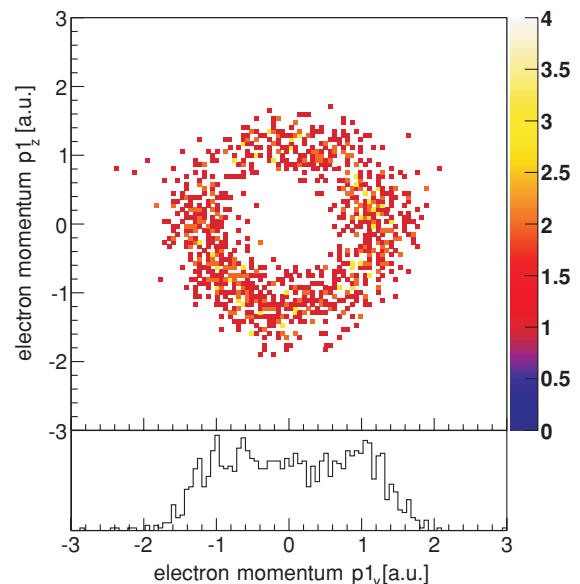

FIG. 7. (Color online) Density plot of the electron momentum correlated with peak (b) in Fig. 3 projected into the plane of circular polarization. The observed donutlike shape is a clear signature of the rotating laser field.

In the second scenario of RCT the laser field would first create Ar^{2+}-Ar. The transfer of one electron then occurs via the overlap of the two electronic wave functions involved [32–34]. Therefore the transfer rate increases exponentially with decreasing R. Due to a charge-induced dipole interaction the Ar^{2+}-Ar exhibits an attractive potential causing the dimer to shrink before—at some smaller internuclear distance—the charge transfer finally leads to a Coulomb explosion. This process has been previously observed in a synchrotron radiation experiment by Saito *et al.* [33,35]. There a one-site doubly charged $Ar^{2+}(3p^{-2})$-Ar state decays into a two-site $Ar^{+}(3p^{-1})$-$Ar^{+}(3p^{-1})$ + hν giving rise to a kinetic energy release of 5.24 to 4.6 eV and a corresponding R of 2.75 to 3.10 Å [21].

We expect the one-site doubly ionized argon dimer to underlie the same double-ionization mechanism as the Ar^{2+} monomer since their ionization thresholds are almost equal (43.46 eV for the Ar^{2+} monomer). As discussed previously, in the intensity regime of our experiment, rescattering is more effective than the sequential double ionization, as the double-hump structure in Fig. 3 and the polarization dependence (Table I) show. In comparison to the monomer, however, Table I shows only a very weak polarization dependence of KER peak (b), ruling out the nonsequential ionization being the precursor for the one-site doubly charged argon dimer. This again is in line with the observed orientation dependence [Fig. 4(b)]. As for the rescattering mechanism, no orientation dependence would be expected. Manschwetus and coworkers [36] suggest a process of laser induced charge transfer in the dimer which produces a one-site double excited state which than decays via RCT giving rise to peak (b). This scenario is consistent with our data.

We now discuss the excitation scenario. Here two-center ionization would have to be accompanied by excitation to a potential energy curve which is much steeper than $1/R$ so that dissociation starting at the ground-state equilibrium distance still produces a higher KER. We did not find published potential energy curves for such highly excited states in the literature, but as the excitation increases toward the triple-ionization threshold, the shape of the repulsive potential energy curves approaches a $2/R$ slope. Thus there could exist one or several states of the type Ar^{+}-Ar^{+*} which produce the kinetic energy release of peak (b).

What is a possible scenario which does not only lead to two-center double-electron emission but to additional excitation? First the excitation could be produced by inelastic recollision of one of the two electrons. As Table I shows there is a small but significant elipticity dependence of peak (b) which indicates that some of the rate of peak (b) is indeed produced by rescattering. However, judging from the elipticity dependence, there must be a second pathway which is open also with circular light. One possibility is that the tunneling of one of the two electrons does not occur from the highest occupied molecular orbital (HOMO) but from a deeper lying orbital. There is increasing evidence that such processes do play a role [37]. Alternatively the excitation might be created by shake-up accompanying tunneling as recently reported [38,39]. A further possibility would be that one of the tunneled electrons undergoes an inelastic collision at the neighbor atom on the way out of the dimer. However, the
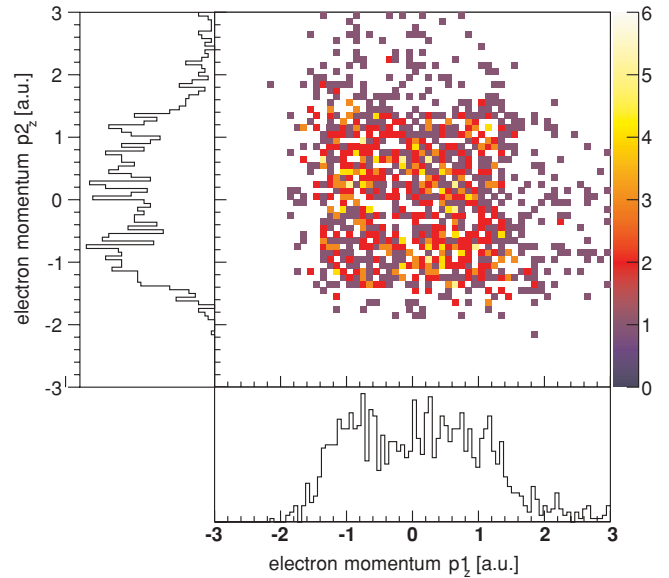

FIG. 8. (Color online) Momentum correlation between the two emitted electrons for circularly polarized light. The time-of-flight momentum component of the first electron is plotted versus the same momentum component of the corresponding second electron. Electrons that are emitted at the same instant need to have the same sign of their momenta.

energy of an electron accumulated in the field over a distance of 3 Å is about 18 eV, barely enough for the excitation which is required. So, if such a process is active the inelastic collision would probably have to be laser assisted, that is, with the need to additionally absorb some photons from the field.

From our data we therefore cannot conclusively identify the mechanism. We can, however, confirm that the two electrons are set free sequentially during the pulse. This is demonstrated by Fig. 8, which shows a correlation map of two electrons measured for circularly polarized light. On the horizontal axis one momentum component (along the time-of-flight axis) of the first electron ($p1_z$) is plotted and on the vertical axis the corresponding distribution for the second electron ($p2_z$) is plotted. We calculated the momentum component for the second electron from momentum conservation including both argon ions as well as the measured electron. This spectrum confirms that there is no time-fixed correlation between the two electrons, both of which show a donut-shaped momentum distribution. They are freed at independent times during the pulse. For comparison, the case of nonsequential double ionization of atoms in linear polarization, the corresponding spectrum, shows peaks in the first and third quadrant [40]. In the rescattering case both electrons are set free upon recollision at the same instant of time and hence receive the same momentum transfer from the field.

C. Peak (c)

The most striking feature of the highest KER peak, peak (c), is its absence in the case of circularly polarized light. Hence, we suspect the dynamics of the electronic wave packet in the field to play a significant role in the process leading to that peak.

For the interpretation of the kinetic energy release at first conclusions similar to those for peak (b) apply: It cannot result from a Coulomb explosion of two singly charged ions on an $1/R$ potential. As the KER is approximately doubled compared to peak (a) the ionization rather has to lead to a potential curve falling like $2/R$. Still the fragmentation of the argon dimer is into two singly charged ions. All highly excited Rydberg states, for which the radius of the orbit of the excited electron is larger than the internuclear distance, will have the required shape of the potential energy curve. The first step producing these states would be the two-site tunnel ionization as for peak (a). Then a third electron would tunnel out via enhanced ionization but would be recaptured upon recollision in a Rydberg state. Tunneling with subsequent trapping of the electron in a highly excited Rydberg state has been recently observed [41]. In this process the electron tunnels through the barrier of the nucleus and can be recaptured in the Coulomb field of the nuclei if the drift energy gained from the laser field is not sufficient for a subsequent ionization [42]. For that mechanism it is mandatory that the laser field is already considerably weakened enabling the excited state to survive. The capture of free electrons in a decreasing laser field is also possible [43]. When an electron is driven back to its parent ion at the tail of the fading pulse its drift energy can be too low to finally escape the Coulomb potential. As the kinetic energy of an electron acquired in circular polarization is independent from the phase and too large to trap the electron, this process does only occur for linearly polarized light. It was termed frustrated tunnel ionization and has been observed in He and H_2 by measuring the excited neutral fragments [41–43].

As indicated in Fig. 1 we also observe the Ar^{2+}-Ar^+ breakup channel, showing clear evidence that the Ar_2^{3+} ionization is possible. It is a precursor for the process underlying channel c.

The angular distribution of the ions [Fig. 4(c)] further confirms our assumption as it is strongly enhanced along the polarization direction. The first ionization step, proceeding via tunneling, is expected to be isotropic, whereas the second tunnel ionization is enhanced along the polarization direction.

As the third step is again enhanced ionization followed by recapturing this will further pronounce the angular distribution along the polarization axis. Frustrated tunnel ionization thus explains both, the absence in the case of circular light and the high KER value of peak (c) matching our experimental results.

V. CONCLUSION

In conclusion, we have shown that the ionization of argon dimers into two singly charged fragments can proceed through different pathways identified by three distinct peaks in the KER distribution. At our laser intensities, the dominant channel is a sequential two-site double ionization giving rise to a kinetic energy of the ions that corresponds to the ground-state internuclear distance of the argon dimer. The weakest channel giving rise to the highest KER was identified as frustrated triple tunnel ionization, a process that generates an excited Rydberg state. For the third process leading to an intermediate KER we can exclude interatomic Coulombic decay and are left with two possible scenarios. The first scenario is a two-site tunnel-ionization which is accompanied by excitation to a potential energy curve substantially steeper than $1/R$. Alternatively our data are also consistent with a laser-induced charge transfer mechanism put forward in [36].

Furthermore, we showed an enhanced ionization probability if the molecular axis is parallel to the electric field. We take that as evidence for a charge-enhanced tunnel-ionization mechanism. In this process the tunneling barrier is suppressed by the joint action of the neighboring charge acting in parallel with the laser field. Due to the large equilibrium distance of the dimer no nuclear dynamics is required for this process to occur which is contrary to covalently bound molecules.

[1] F. M. Tao and Y. K. Pan, Mol. Phys. **81**, 507 (1994).

[2] K. Patkowski, G. Murdachaew, C. Fou, and K. Szalewicz, Mol. Phys. **103**, 2031 (2005).

[3] R. Dörner, Th. Weber, M. Weckenbrock, A. Staudte, M. Hattass, H. Schmidt-Böcking, R. Moshammer, and J. Ullrich, Adv. At. Mol. Opt. Phys. **48** (2002).

[4] A. Becker, R. Dörner, and R. Moshammer, J. Phys. B **38**, S753 (2005).

[5] P. B. Corkum, Phys. Rev. Lett. **71**, 1994 (1993).

[6] T. Seideman, M. Yu. Ivanov, and P. B. Corkum, Phys. Rev. Lett. **75**, 2819 (1995).

[7] T. Zuo and A. D. Bandrauk, Phys. Rev. A **52**, R2511 (1995).

[8] J. H. Posthumus, J. Plumridge, P. F. Taday, J. H. Sanderson, A. J. Langley, K. Codling, and W. A. Bryan, J. Phys. B **32**, L93 (1999).

[9] Th. Weber *et al.*, J. Phys. A **33**, L127 (2000).

[10] A. S. Alnaser, X. M. Tong, T. Osipov, S. Voss, C. M. Maharjan, B. Shan, Z. Chang, and C. L. Cocke, Phys. Rev. A **70**, 023413 (2004).

[11] I. V. Litvinyuk, K. F. Lee, P. W. Dooley, D. M. Rayner, D. M. Villeneuve, and P. B. Corkum, Phys. Rev. Lett. **90**, 233003 (2003).

[12] J. Ullrich, R. Moshammer, R. Dörner, O. Jagutzki, V. Mergel, H. Schmidt-Böcking, and L. Spielberger, J. Phys. B **30**, 2917 (1997).

[13] R. Dörner, V. Mergel, O. Jagutzki, L. Spielberger, J. Ullrich, R. Moshammer, and H. Schmidt-Böcking, Phys. Rep. **330**, 95 (2000).

[14] O. Jagutzki *et al.*, IEEE Trans. Nucl. Sci. **49**, 2477 (2002).

[15] B. Walker, B. Sheehy, L. F. DiMauro, P. Agostini, K. J. Schafer, and K. C. Kulander, Phys. Rev. Lett. **73**, 1227 (1994).

[16] P. Dietrich, N. H. Burnett, M. Ivanov, and P. B. Corkum, Phys. Rev. A **50**, R3585 (1994).

[17] Th. Weber *et al.*, Phys. Rev. Lett. **84**, 443 (2000).

[18] R. Moshammer *et al.*, Phys. Rev. Lett. **84**, 447 (2000).

[19] A. Staudte *et al.*, Phys. Rev. Lett. **102**, 033004 (2009).

[20] S. P. Goreslavski, G. G. Paulus, S. V. Popruzhenko, and N. I. Shvetsov-Shilovski, Phys. Rev. Lett. **93**, 233002 (2004).

[21] S. D. Stoychev, A. I. Kuleff, F. Tarantelli, and L. S. Cederbaum, J. Chem. Phys. **128**, 014307 (2008).

[22] L. S. Cederbaum, J. Zobeley, and F. Tarantelli, Phys. Rev. Lett. **79**, 4778 (1997).

[23] S. Marburger, O. Kugeler, U. Hergenhahn, and T. Möller, Phys. Rev. Lett. **90**, 203401 (2003).

[24] T. Jahnke *et al.*, Phys. Rev. Lett. **93**, 163401 (2004).

[25] T. Aoto, K. Ito, Y. Hikosaka, E. Shigemasa, F. Penent, and P. Lablanquie, Phys. Rev. Lett. **97**, 243401 (2006).

[26] Y. Morishita *et al.*, Phys. Rev. Lett. **96**, 243402 (2006).

[27] T. Havermeier *et al.*, Phys. Rev. Lett. **104**, 133401 (2010).

[28] R. Santra and L. S. Cederbaum, Phys. Rev. Lett. **90**, 153401 (2003).

[29] R. Santra and L. S. Cederbaum, Phys. Rev. Lett. **94**, 199901(E) (2005).

[30] K. Kreidi *et al.*, Phys. Rev. Lett. **103**, 033001 (2009).

[31] P. B. Corkum, N. H. Burnett, and F. Brunel, Phys. Rev. Lett. **62**, 1259 (1989).

[32] T. Jahnke *et al.*, Phys. Rev. Lett. **99**, 153401 (2007).

[33] N. Saito, Y. Morishita, I. H. Suzuki, S. D. Stoychev, A. I. Kuleff, L. S. Cederbaum, X.-J. Liu, H. Fukuzawa, G. Prümper, and K. Ueda, Chem. Phys. Lett. **441**, 16 (2007).

[34] K. Kreidi *et al.*, Phys. Rev. A **78**, 043422 (2008).

[35] K. Ueda, X.-J. Liu, G. Prümper, H. Fukuzawa, Y. Morishita, and N. Saito, J. Electron Spectrosc. Relat. Phenom. **155**, 113 (2007).

[36] B. Manschwetus, H. Rottke, G. Steinmeyer, L. Foucar, A. Czasch, H. Schmidt-Böcking, and W. Sandner, Phys. Rev. A **82**, 013413 (2010).

[37] H. Akagi, T. Otobe, A. Staudte, A. Shiner, F. Turner, R. Dörner, D. M. Villeneuve, and P. B. Corkum, Science **325**, 1364 (2009).

[38] I. V. Litvinyuk, F. Legare, P. W. Dooley, D. M. Villeneuve, P. B. Corkum, J. Zanghellini, A. Pegarkov, C. Fabian, and T. Brabec, Phys. Rev. Lett. **94**, 033003 (2005).

[39] W. A. Bryan *et al.*, Nature Phys. **2**, 379 (2006).

[40] Th. Weber, H. Giessen, M. Weckenbrock, G. Urbasch, A. Staudte, L. Spielberger, O. Jagutzki, V. Mergel, M. Vollmer, and R. Dörner, Nature (London) **405**, 658 (2000).

[41] T. Nubbemeyer, K. Gorling, A. Saenz, U. Eichmann, and W. Sandner, Phys. Rev. Lett. **101**, 233001 (2008).

[42] B. Manschwetus, T. Nubbemeyer, K. Gorling, G. Steinmeyer, U. Eichmann, H. Rottke, and W. Sandner, Phys. Rev. Lett. **102**, 113002 (2009).

[43] U. Eichmann, T. Nubbemeyer, H. Rottke, and W. Sandner, Nature (London) **461**, 1261 (2009).